Plasticity in growth behavior of patients' acute myeloid leukemia stem cells growing in mice

Sarah Ebinger,[1] Christina Zeller,[1] Michela Carlet,[1] Daniela Senft,[1] Johannes W. Bagnoli,[2] Wen-Hsin Liu,[1] Maja Rothenberg-Thurley,[3] Wolfgang Enard,[2] Klaus H. Metzeler,[3-5] Tobias Herold,[1,3,4] Karsten Spiekermann,[3-5] Binje Vick[1,4] and Irmela Jeremias[1,4,6]

[1]Research Unit Apoptosis in Hematopoietic Stem Cells, Helmholtz Zentrum München, German Research Center for Environmental Health (HMGU), Munich; [2]Anthropology & Human Genomics, Department of Biology II, Ludwig-Maximilians-University, Martinsried, Germany; [3]Laboratory for Leukemia Diagnostics, Department of Medicine III, University Hospital, Ludwig-Maximilians-University Munich, Munich; [4]German Cancer Consortium (DKTK), partner site Munich; [5]German Cancer Research Center (DKFZ), Heidelberg and [6]Department of Pediatrics, Dr. von Hauner Childrens Hospital, Ludwig Maximilian University, Munich, Germany

Correspondence: IRMELA JEREMIAS - Irmela.Jeremias@helmholtz-muenchen.de

doi:10.3324/haematol.2019.226282

Plasticity in growth behavior of patients' acute myeloid leukemia stem cells growing in mice

Sarah Ebinger[1], Christina Zeller[1], Michela Carlet[1], Daniela Senft[1], Johannes Bagnoli[2], Wen-Hsin Liu[1], Maja Rothenberg-Thurley[3], Wolfgang Enard[2], Klaus H. Metzeler[3-5], Tobias Herold[1,3-5], Karsten Spiekermann[3-5], Binje Vick[1,4], Irmela Jeremias[1,4,5]

Supplemental Information

This pdf file contains:

Supplemental Methods and References
Supplemental Tables (3)
Supplemental Figures (5)

Supplemental Methods

Patients' acute myeloid leukemia (AML) cells

Bone marrow (BM) or peripheral blood (PB) samples from adult AML patients were obtained from the Department of Internal Medicine III, Ludwig-Maximilians-Universität, Munich, Germany, during the years 2012 and 2014. Specimens were collected for diagnostic purposes before start of treatment. Written informed consent was obtained from all patients. The study was performed in accordance with the ethical standards of the responsible committee on human experimentation (written approval by the Research Ethics Boards of the medical faculty of Ludwig-Maximilians-Universität, Munich, number 068-08 and 222-10) and with the Helsinki Declaration of 1975, as revised in 2000. AML-538 was kindly provided by Claudia Baldus and Lorenz Bastian (Charité Universitätsmedizin Berlin, Germany). Pediatric AML PDX samples were a gift from Maya C. André and Martin Ebinger (University Children's Hospital Tuebingen, Germany), and were described previously.(1) Genetic profiling of AML PDX and primary AML samples was performed by Maja Rothenberg-Thurley and Klaus H. Metzeler, as described previously.(2)

The patient derived xenograft (PDX) mouse model of patients' AML

Xenotransplantation and establishing AML PDX cells in NSG mice (NOD-*scid*-gamma, The Jackson Laboratory, Bar Harbour, ME, USA) was performed as described previously.(3) In the study presented here, only AML PDX cells were applied that re-engrafted in NSG mice over several passages, and lead to a BM chimerism above 90% $hCD33^+$ $hCD45^+$ cells within 16 weeks after transplantation. These requirements precluded the use of primary patient cells, slow engrafters, low engrafters, or samples without the capacity to re-engraft; therefore, the PDX cohort used in this study is enriched for highly aggressive samples. All animal trials were

performed in accordance with the current ethical standards of the official committee on animal experimentation (written approval by Regierung von Oberbayern, tierversuche@reg-ob.bayern.de; 55.2-1-54-2531-95-10, ROB-55.2Vet-2532.Vet_02-15-193, ROB-55.2Vet-2532.Vet_02-16-7 and ROB-55.2Vet-2532.Vet_03-16-56). Accuracy of sample identity was verified by repetitive finger printing using PCR of mitochondrial DNA.(4)

Lentiviral transduction of AML PDX cells and enrichment of transgenic cells

In vitro culture, lentiviral constructs, transduction, and sorting of transgenic PDX cells were performed as described previously.(3) In the study presented here, cells were transduced with a construct expressing enhanced firefly luciferase and mCherry in equimolar amounts (pCDH-EF1a-eFFly-mCherry, available via Addgene #104833). Initial lentiviral transduction efficiencies were between 1% and 44% (AML-346 30%, AML-372 1%, AML-388 2%, AML-393 12%, AML-491 11%, AML-579 1%, AML-661 44%). PDX cells were sorted using a FACSAria III (BD Biosciences, Heidelberg, Germany) to reach a purity of more than 95% of $mCherry^+$ cells. As control, three AML PDX samples without transgenic expression of firefly luciferase and mCherry were applied (AML-356, AML-358, AML-538).

Bioluminescence *in vivo* imaging (BLI)

BLI and quantification of tumor burden was performed as described previously.(3, 5)

Labeling of PDX cells with carboxyfluorescein succinimidyl ester (CFSE)

Labeling of PDX cells with CFSE was performed as described previously.(5) In brief, AML PDX cells were isolated from mice with advanced disease stage, indicated by a BM chimersim of more than 90% $mCherry^+$ PDX cells. Cells were labeled with CFSE *ex vivo* (Life Technologies, Carlsbad, CA, USA) according to manufacturer's

instructions, washed in PBS, and injected into next recipient mice (10^7 $CFSE^+$ PDX cells per mouse). The procedure resulted in CFSE positivity of well above 98% of PDX cells, as validated by flow cytometry. As AML PDX cells are heterogeneous in size, loss of CFSE appears as continuum in flow cytometry, devoid of the distinct peaks known from normal leukocytes.

Enriching and quantifying PDX and label-retaining cells (LRC) from mouse BM

To purify AML PDX cells from mouse BM, bones from hip, femura, tibiae, sternum and spine were crushed with a mortar and pistil, cells were washed once in PBS, and filtered through a cell strainer (EASYSTRAINER 70 µM, Greiner bio-one, Frickenhausen, Germany). Murine cells were depleted using magnetic beads according to manufacturer's instructions (Mouse Cell Depletion Kit, Miltenyi Biotech, Bergisch Gladbach, Germany), with the exception that only 100 µl MicroBeads and two columns were used for one mouse BM suspension. As second step, AML PDX cells were analyzed or sorted by flow cytometry by gating on (i) leukocytes in FSC/SSC, and (ii) $DAPI^-$ living cells and transgenic $mCherry^+$ AML PDX cells using a BD LSRFortessa or FACSAriaIII, respectively (BD Biosciences, Heidelberg, Germany) as shown in Figure **1B**. Sorting of LRC and non-LRC was performed with the precision setting "purity" at the FACSAria. To determine the fraction of low-cycling AML PDX cells, LRC were discriminated from non-LRC using CFSE staining as shown in Figure **1B.** To quantify LRC, CFSE mean fluorescence intensity (MFI) of CFSE labelled PDX cells either incubated for two to three days *ex vivo* or isolated from a mouse two to three days after injection was measured, which defined the starting condition (''0 divisions''). Day two or three CFSE MFI was divided by factor two to calculate putative CFSE bisections mimicking cell divisions. Cells with a high CFSE signal below three bisections of the maximum CFSE MFI were defined as

LRC. Seven CFSE MFI bisections or more were defined as entire loss of the CFSE signal characterizing non-LRC. At late time points, due to high cell numbers and time-dependent issues, after murine cell depletion often 1/10 of cells were analyzed by flow cytometry. Absolute cell numbers were calculated thereof.

Cell cycle analysis

AML PDX cells were isolated from a first donor mouse, labeled with CFSE and 10^7 cells were transplanted into first recipients. Sixteen days after injection, AML PDX cells were re-isolated as described above. After Mouse Cell Depletion Kit, cells were stained with Vibrant DyeCycle Violet (Invitrogen, Eugene, OR, USA) according to manufacturer's instructions. Cells were analyzed by flow cytometry for cell cycle distribution within the LRC and non-LRC compartment.

RNA sequencing and data analysis

Library Preparation of RNA-Seq: 1,000 and 2,000 cells of each individual sample were sorted and lysed in RLT Plus (Qiagen) supplemented with 1% 2-Mercaptoethanol (Sigma Aldrich) and stored at -80°C until processing. A modified SCRB-seq protocol (6, 7) was used for library preparation. Briefly, proteins in the lysate were digested by Proteinase K (Ambion), RNA was cleaned up using SPRI beads (GE, 22% PEG). In order to remove isolated DNA, samples were treated with DNase I for 15 min at RT. cDNA was generated by oligo-dT primers containing well specific (sample specific) barcodes and unique molecular identifiers (UMIs). Unincorporated barcode primers were digested using Exonuclease I (Thermo Fisher). cDNA was pre-amplified using KAPA HiFi HotStart polymerase (Roche) and pooled before Nextera libraries were constructed from 0.8 ng of pre-amplified cleaned up cDNA using Nextera XT Kit (Illumina). 3' ends were enriched with a custom P5 primer (P5NEXTPT5, IDT) and libraries were size selected using 2% E-

Gel Agarose EX Gels (Life Technologies), cut out in the range of 300–800 bp, and extracted using the Monarch DNA Gel Extraction Kit (New England Biolabs) according to manufacturer's recommendations.

Sequencing: Libraries were paired-end sequenced on a rapid flow cell (1.5 lanes, ~208*10^6 reads in total) of an Illumina HiSeq 1500 instrument. Sixteen bases were sequenced within the first read to obtain cellular and molecular barcodes, and 50 bases were sequenced in the second read into the cDNA fragment. An additional eight bases were sequenced to obtain the i7 barcode.

Data processing and differential gene expression and pathway analysis: All raw fastq data was demultiplexed using deML (8) and further processed with zUMIs (9). Mapping was performed using STAR 2.6.0a (10) against the concatenated human (hg38) and mouse genome (mm10). Gene annotations were obtained from Ensembl (GRCh38.84/GRCm38.75). Samples were identified via the cellular barcode, with initial phred score filtering allowing one base below 20. UMI phred filtering allowed one bases below phred 20. Differential gene expression of LRC and nLRC was calculated using the DESeq2 package following recommended workflows.(11) Pathway analysis using the MSigDB Collection "hallmark of cancer" and "KEGG" (v7.0) was conducted using default setting.(12, 13) Sequencing data are available at the NCBI Gene Expression Omnibus (GEO accession number: GSE141627).

In vivo treatment trials

AML PDX cells were injected into groups of mice (10^7 $CFSE^+$ PDX cells per mouse). Seven days after cell injection, mice were treated with a combination of Cytarabine (150 mg/kg dissolved in PBS, i.p.) on days seven, eight, and nine, and one dose of DaunoXome (20 mg/kg i.v.) on day seven (see scheme in Figure **2A**). Body weight was measured daily. Tumor burden was monitored on days seven and ten by BLI. At

day ten, mice were sacrificed, BM was collected, and AML PDX cells were isolated and analyzed for CFSE label retention as described above.

Analysis of plasticity of LRC and non-LRC

AML PDX cells were isolated from a first donor mouse, labeled with CFSE and transplanted into first recipient mice as described above. Ten (AML-393) or 15 (AML-491) days after injection, AML PDX cells were re-isolated and purely sorted into LRC and non-LRC fractions as described above (see also scheme in Figures **3** and **S4**). Limiting dilutions of sorted cells were re-injected into secondary recipient mice (between 30 and 3000 cells per mouse, see **Table S3**). Tumor outgrowth was analyzed by BLI and compared between the groups. Engraftment was determined by positive bioluminescence in vivo imaging signal, analysis of $hCD33^+/hCD45^+$ cells in peripheral blood (PB), and/or analysis of $hCD33^+/hCD45^+$ cells in BM by FACS staining. If no AML PDX cells were detectable within 150 days after injection via BLI, in PB or in BM, mice were counted as non-engrafters. LIC frequencies were determined according to Poisson statistics, using the ELDA software application (http://bioinf.wehi.edu.au/software/elda/).(14)

To determine if highly proliferative cells convert into low-cycling cells, non-LRC from a primary recipient mouse were isolated at day 20 (AML-393) or 21 (AML-491), sorted, re-labeled with CFSE, and re-injected into secondary recipient mice ($3.6*10^6$ $CFSE^+$ AML-393 non-LRC, n=8, or $1.9*10^6$ $CFSE^+$ AML-491 non-LRC, n=5). Cells were re-isolated at different time points after injection, distribution of LRC and non-LRC was analyzed, and compared to the distribution within first recipient mice.

For this analysis, many cells are needed for the re-injection into secondary recipient mice. The minute numbers of LRC that can be re-isolated after ten days from first recipient mice cannot be enriched from secondary recipient mice after re-

transplantation; therefore, it is technically unfeasible to perform this analysis with the LRC fraction of cells.

Analysis of CD34 and CD38 immunophenotype

AML PDX cells were isolated from a first donor mouse, labeled with CFSE and 10^7 cells were transplanted into first recipients. Ten (AML-393) or 14 (AML-491) days after injection, AML PDX cells were re-isolated as described above. After Mouse Cell Depletion Kit, 19/20 of cells were stained with 10 µl PC7-conjugated CD34 monoclonal antibody 581 (Beckman Coulter,Marseille, France) and 10 µl APC-conjugated CD38 monoclonal antibody HIT2 (BioLegend, San Diego, CA, USA). In the remaining 1/20 of cells, antibody-reactivity was controlled using 5 µl isotype-matched control-antibodies. For detection of CD34+/CD38- cells within the LRC and non-LRC compartment, cells were analyzed by flow cytometry.

Statistics

Statistical analyses were calculated using GraphPad Prism 7 software. To compare groups after drug treatment, we first checked normality in the control and treatment group of each sample using the Shapiro-Wilk normality test. If normality assumption was rejected, the Mann Whitney U test was applied. Otherwise, variance homogeneity was tested using the F test, and based on these results, we applied the students or welchs t-test as appropriate. Due to the explorative nature and the limited statistical power based on small sample size, we decided not to correct for multiple testing with respect to tumor samples. ELDA software was used to test differences in LIC frequency by chi-square test (http://bioinf.wehi.edu.au/software/elda/).(14)

References

1. Woiterski J, Ebinger M, Witte KE, Goecke B, Heininger V, Philippek M, et al. Engraftment of low numbers of pediatric acute lymphoid and myeloid leukemias into NOD/SCID/IL2Rcgammanull mice reflects individual leukemogenecity and highly correlates with clinical outcome. International journal of cancer. 2013 Oct 1;133(7):1547-56.

2. Metzeler KH, Herold T, Rothenberg-Thurley M, Amler S, Sauerland MC, Görlich D, et al. Spectrum and prognostic relevance of driver gene mutations in acute myeloid leukemia. Blood. 2016;128(5):686.

3. Vick B, Rothenberg M, Sandhofer N, Carlet M, Finkenzeller C, Krupka C, et al. An advanced preclinical mouse model for acute myeloid leukemia using patients' cells of various genetic subgroups and in vivo bioluminescence imaging. PloS one. 2015;10(3):e0120925.

4. Hutter G, Nickenig C, Garritsen H, Hellenkamp F, Hoerning A, Hiddemann W, et al. Use of polymorphisms in the noncoding region of the human mitochondrial genome to identify potential contamination of human leukemia-lymphoma cell lines. The hematology journal : the official journal of the European Haematology Association. 2004;5(1):61-8.

5. Ebinger S, Ozdemir EZ, Ziegenhain C, Tiedt S, Castro Alves C, Grunert M, et al. Characterization of Rare, Dormant, and Therapy-Resistant Cells in Acute Lymphoblastic Leukemia. Cancer Cell. 2016 Dec 12;30(6):849-62.

6. Soumillon M, Cacchiarelli D, Semrau S, van Oudenaarden A, Mikkelsen TS. Characterization of directed differentiation by high-throughput single-cell RNA-Seq. bioRxiv. 2014:003236.

7. Ziegenhain C, Vieth B, Parekh S, Reinius B, Guillaumet-Adkins A, Smets M, et al. Comparative Analysis of Single-Cell RNA Sequencing Methods. Molecular cell. 2017 Feb 16;65(4):631-43.e4.

8. Renaud G, Stenzel U, Maricic T, Wiebe V, Kelso J. deML: robust demultiplexing of Illumina sequences using a likelihood-based approach. Bioinformatics (Oxford, England). 2015 Mar 1;31(5):770-2.

9. Parekh S, Ziegenhain C, Vieth B, Enard W, Hellmann I. zUMIs - A fast and flexible pipeline to process RNA sequencing data with UMIs. GigaScience. 2018 Jun 1;7(6).

10. Dobin A, Davis CA, Schlesinger F, Drenkow J, Zaleski C, Jha S, et al. STAR: ultrafast universal RNA-seq aligner. Bioinformatics (Oxford, England). 2013 Jan 1;29(1):15-21.

11. Love MI, Huber W, Anders S. Moderated estimation of fold change and dispersion for RNA-seq data with DESeq2. Genome biology. 2014;15(12):550.

12. Mootha VK, Lindgren CM, Eriksson KF, Subramanian A, Sihag S, Lehar J, et al. PGC-1alpha-responsive genes involved in oxidative phosphorylation are coordinately downregulated in human diabetes. Nature genetics. 2003 Jul;34(3):267-73.

13. Subramanian A, Tamayo P, Mootha VK, Mukherjee S, Ebert BL, Gillette MA, et al. Gene set enrichment analysis: a knowledge-based approach for interpreting genome-wide expression profiles. Proceedings of the National Academy of Sciences of the United States of America. 2005 Oct 25;102(43):15545-50.

14. Hu Y, Smyth GK. ELDA: Extreme limiting dilution analysis for comparing depleted and enriched populations in stem cell and other assays. Journal of Immunological Methods. 2009 2009/08/15/;347(1):70-8.

Table S1. Clinical characteristics of AML patients

Sample	disease stage*	age[1] [years]	sex	cytogenetics	mutations[2]
AML-346	R1	1	f	int. del(5q)(13q)	CKIT
AML-356	R1	5	m	*ND*	*ND*
AML-358	R2	9	m	*ND*	FLT3-TKD
AML-372	R1	42	m	complex, incl. -17	KRAS, TP53
AML-388	ID	57	m	KMT2A-AF6	KRAS, CEBPZ
AML-393	R1	47	f	KMT2A-AF10	BCOR, KRAS
AML-491	R1	53	f	del(7)(q2?1)	DNMT3A, BCOR, NRAS, KRAS, ETV6, PTPN11, RUNX1
AML-538	R1	68	f	CN	DNMT3A, IDH1
AML-579	R1	51	m	CN	NPM1, FLT3-ITD, DNMT3A, IDH1
AML-661	R2	55	f	del(7)(q2?1)	DNMT3A, BCOR, NRAS, ETV6, PTPN11, RUNX1, EZH2

[1]when the primary AML sample was obtained; [2]mutations detected by targeted re-sequencing in PDX cells; ID = initial diagnosis; R1 = 1st relapse; R2 = 2nd relapse; int = interstitial; del = deletion; CN = cytogenetically normal; f = female; m = male; *ND* = not determined

Table S2: LIC frequencies of different AML PDX samples (Related to Figure **S1D**)

Sample	# of cells*	# of mice injected / engrafted	LIC frequency (95% CI)
AML-372	100,000	3 / 3	**1/5,125** (1/1,926 - 1/13,640)
	30,000	3 / 3	
	10,000	3 / 3	
	3,000	3 / 1	
	1,000	3 / 0	
AML-388	72,000	1 / 1	**1/3,665** (1/939 - 1/14,300)
	24,000	1 / 1	
	21.870	1 / 1	
	7,290	1 / 1	
	2,430	2 / 1	
	710	1 / 0	
	270	2 / 0	
	90	1 / 0	
	30	2 / 0	
AML-346	100,000	4 / 4	**1/2,337** (1/898 - 1/6,093)
	20,000	3 / 3	
	10,000	4 / 4	
	2,000	3 / 2	
	1,000	4 / 1	
	100	4 / 0	
AML-491	10,000	3 / 3	**1/1,799** (1/945 - 1/3,426)
	5,400	2 / 2	
	2,000	2 / 1	
	1,800	2 / 0	
	1,200	6 / 6	
	1,000	2 / 1	
	600	5 / 0	
	200	3 / 0	
	100	4 / 0	
AML-393	20,000	3 / 3	**1/507** (1/194-1/1,325)
	2,000	3 / 3	
	666	3 / 1	
	200	3 / 2	
	66	3 / 1	
AML-579	72,900	1 / 1	**1/351** (1/77.6-1/1,590)
	24,300	2 / 2	
	7,100	1 / 1	
	2,700	2 / 2	
	900	1 / 1	
	300	2 / 1	
AML-661	8,100	1 / 1	**1/546** (1/230 - 1/1,403)
	2,700	1 / 1	
	900	1 / 3	
	300	1 / 3	
	100	2 / 4	
	33	2 / 4	
	11	0 / 3	

*Cells from different AML samples were transplanted into recipient mice in limiting dilutions at numbers indicated; bioluminescence *in vivo* imaging, blood measurement or bone marrow FACS staining was performed to determine engraftment; LIC frequency was calculated using the ELDA software; 95% confidence interval (CI).

Table S3: LIC frequencies of LRC and nLRC (Related to Figure **3B** and **S4B**)

Sample	group	# of cells	# of mice injected / engrafted	LIC frequency (95% CI)
AML-393	non-LRC	3,000	1 / 1	**1/352** (1/157 - 1/788)
		1,480	2 / 1	
		1,400	1 / 1	
		1,000	2 / 2	
		330	2 / 2	
		300	2 / 2	
		200	2 / 1	
		100	3 / 1	
		30	3 / 1	
	LRC	1,500	1 / 1	**1/132** (1/59 - 1/294)
		1,480	2 / 2	
		1,400	1 / 1	
		1,000	1 / 1	
		900	2 / 2	
		330	2 / 1	
		300	3 / 3	
		200	2 / 2	
		100	2 / 2	
		30	3 / 0	
AML-491	non-LRC	2,000	1 / 1	**1/1,080** (1/336 - 1/3,474)
		1,200	2 / 2	
		950	1 / 0	
		600	1 / 0	
	LRC	2,000	1 / 1	**1/1,021** (1/324 - 1/3,225)
		1,200	2 / 2	
		600	2 / 0	
		200	1 / 0	

*LRC and non-LRC from first recipient mice were sorted and were transplanted into secondary recipient mice in limiting dilutions at numbers indicated; bioluminescence *in vivo* imaging, blood measurement or bone marrow FACS staining was performed to determine engraftment; LIC frequency was calculated using the ELDA software; 95% confidence interval (CI).

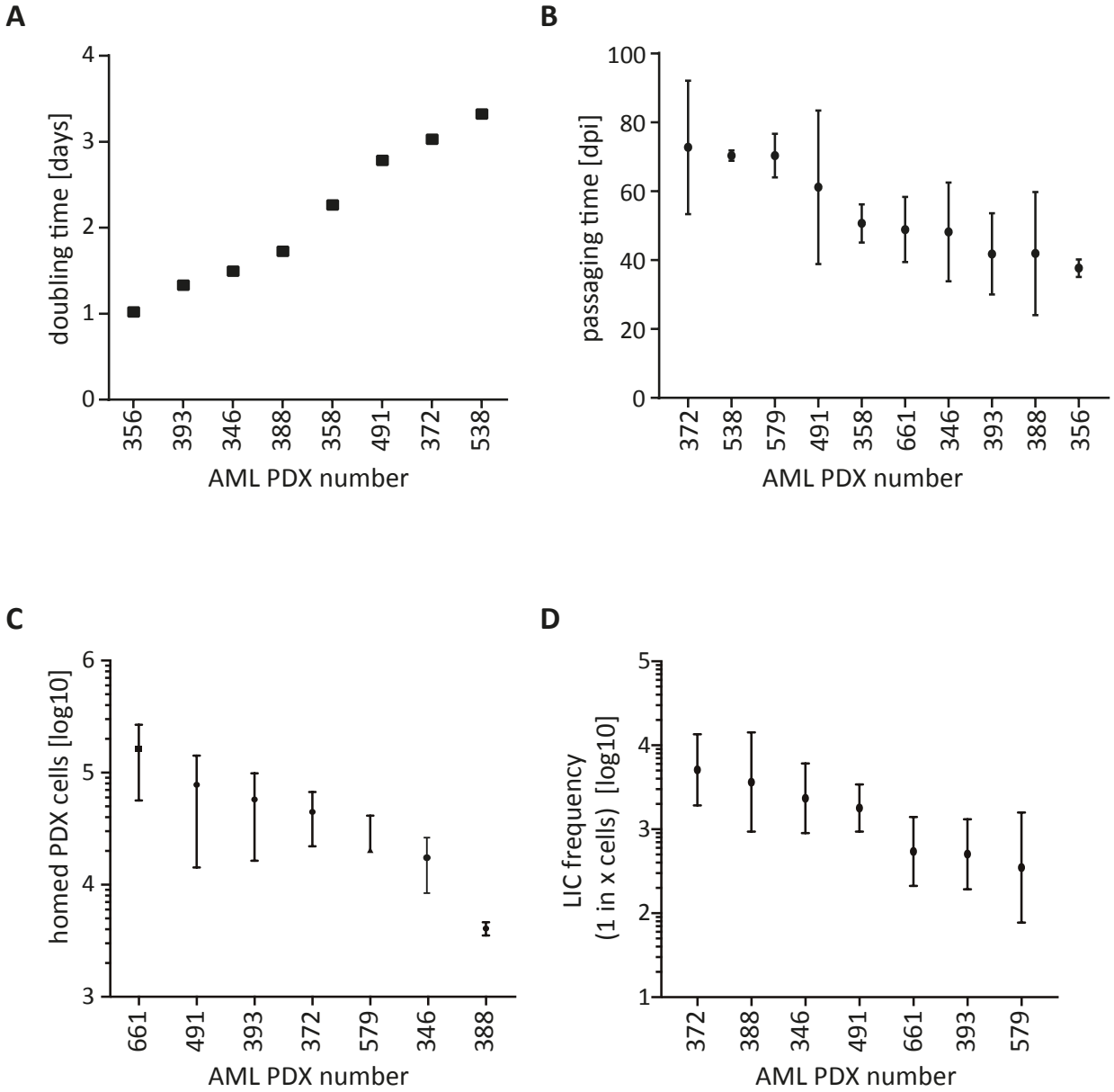

Figure S1 AML PDX cells display heterogeneity regarding *in vivo* proliferation, homing and LIC frequency (related to Figure **1**).

A *In vivo* doubling times were calculated out of growth curves measured as in Figures **1D** and **S2**.

B Passaging times from injection until overt leukemia, $5x10^5$ to $5x10^6$ AML PDX cells were injected per mouse; mean +/- SD of at least 4 and up to 100 mice per sample is depicted. dpi=days post injection.

C Number of AML PDX cells homing to the BM was determined 2 or 3 days following injection of 10^7 cells; mean +/- SD of at least 3 mice is shown.

D Bulk cells from different AML samples were transplanted into recipient mice in limiting dilutions at numbers indicated in Table **S2**. LIC frequency was calculated using the ELDA software and mean +/- 95%CI is depicted.

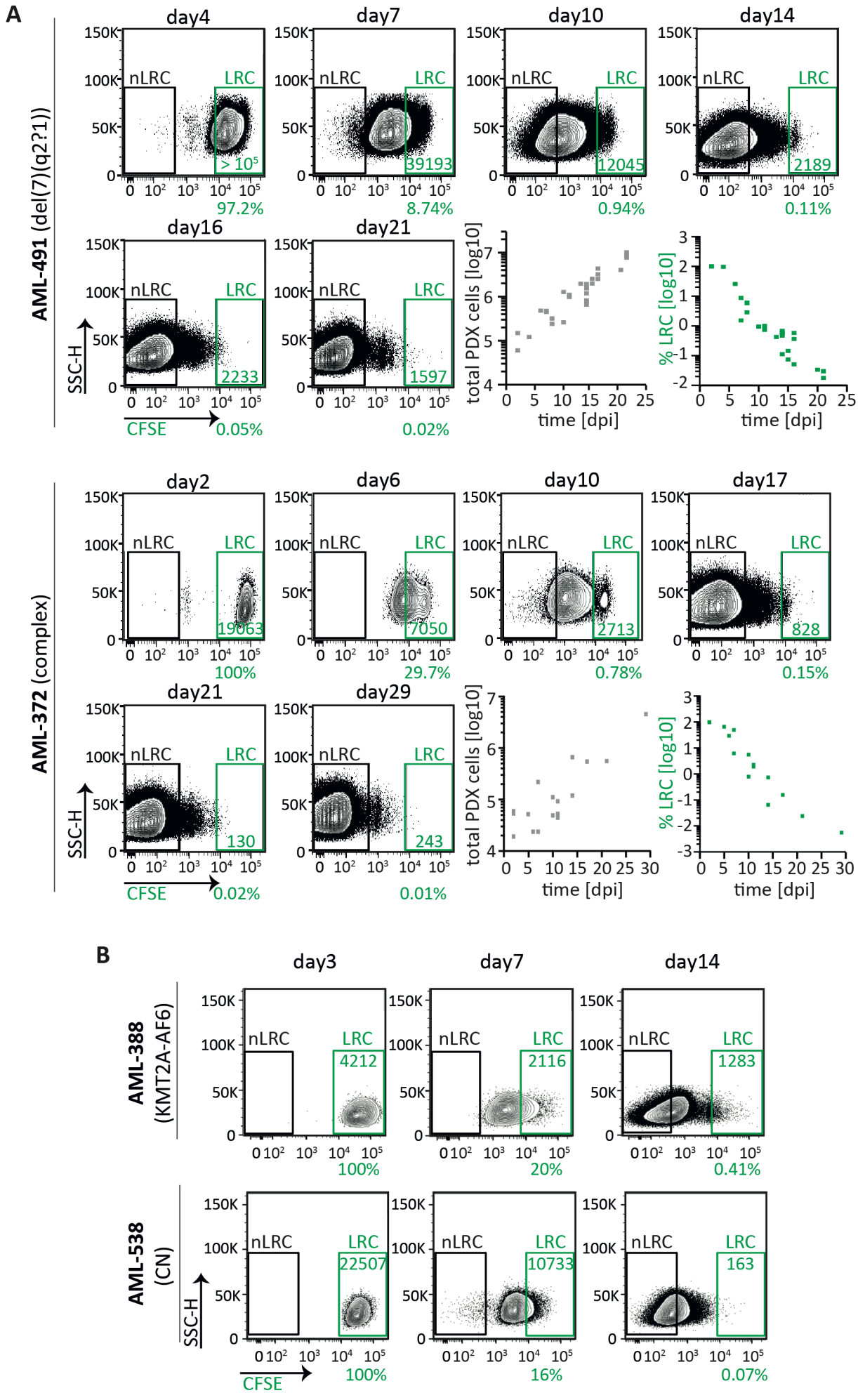
A
AML-491 (del(7)(q2?1))
day4
day7
day10
day14
day16
day21
nLRC
LRC
> 10⁵
39193
12045
2189
2233
1597
97.2%
8.74%
0.94%
0.11%
0.05%
0.02%
SSC-H
CFSE
total PDX cells [log10]
% LRC [log10]
time [dpi]
AML-372 (complex)
day2
day6
day10
day17
day21
day29
19063
7050
2713
828
130
243
100%
29.7%
0.78%
0.15%
0.02%
0.01%
B
AML-388
(KMT2A-AF6)
day3
day7
day14
4212
2116
1283
100%
20%
0.41%
AML-538
(CN)
22507
10733
163
100%
16%
0.07%

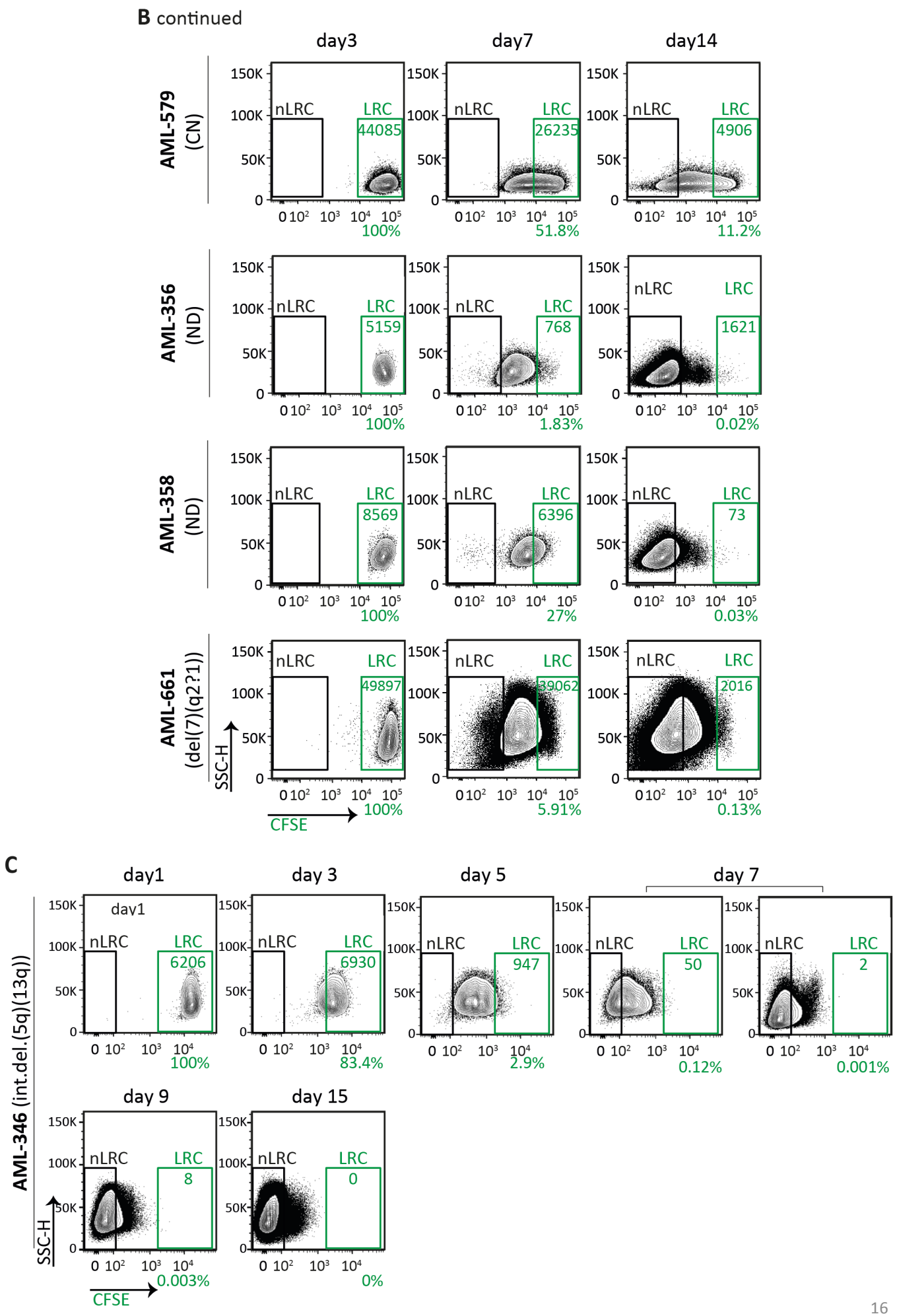
B continued
day3
day7
day14
AML-579 (CN)
AML-356 (ND)
AML-358 (ND)
AML-661 (del(7)(q2?1))
nLRC
LRC
44085
26235
4906
5159
768
1621
8569
6396
73
49897
39062
2016
100%
51.8%
11.2%
100%
1.83%
0.02%
100%
27%
0.03%
100%
5.91%
0.13%
SSC-H
CFSE
C
day1
day 3
day 5
day 7
day 9
day 15
AML-346 (int.del.(5q)(13q))
6206
6930
947
50
2
8
0
100%
83.4%
2.9%
0.12%
0.001%
0.003%
0%

Figure S2 AML PDX cells contain a rare subpopulation of lowly-cycling cells (related to Figure **1,** additional samples).

Experiments were performed and depicted identically as in Figure **1**. In brief, 10^7 CFSE labeled AML PDX cells were injected into groups of mice; cells were isolated at different time points and analyzed by flow cytometry for CFSE content. FACS plots for representative mice are shown. Total number of isolated PDX cells and percentage of LRC cells among all isolated PDX cells are shown in (**A**). Total number of mice studied was (**A**) 30 for AML-491, 18 for AML-372, (**B**) 5 for AML-388, 3 for AML-538, 8 for AML-579, 3 for AML-356, 3 for AML-358, 8 for AML-661 and (**C**) 10 for AML-346.

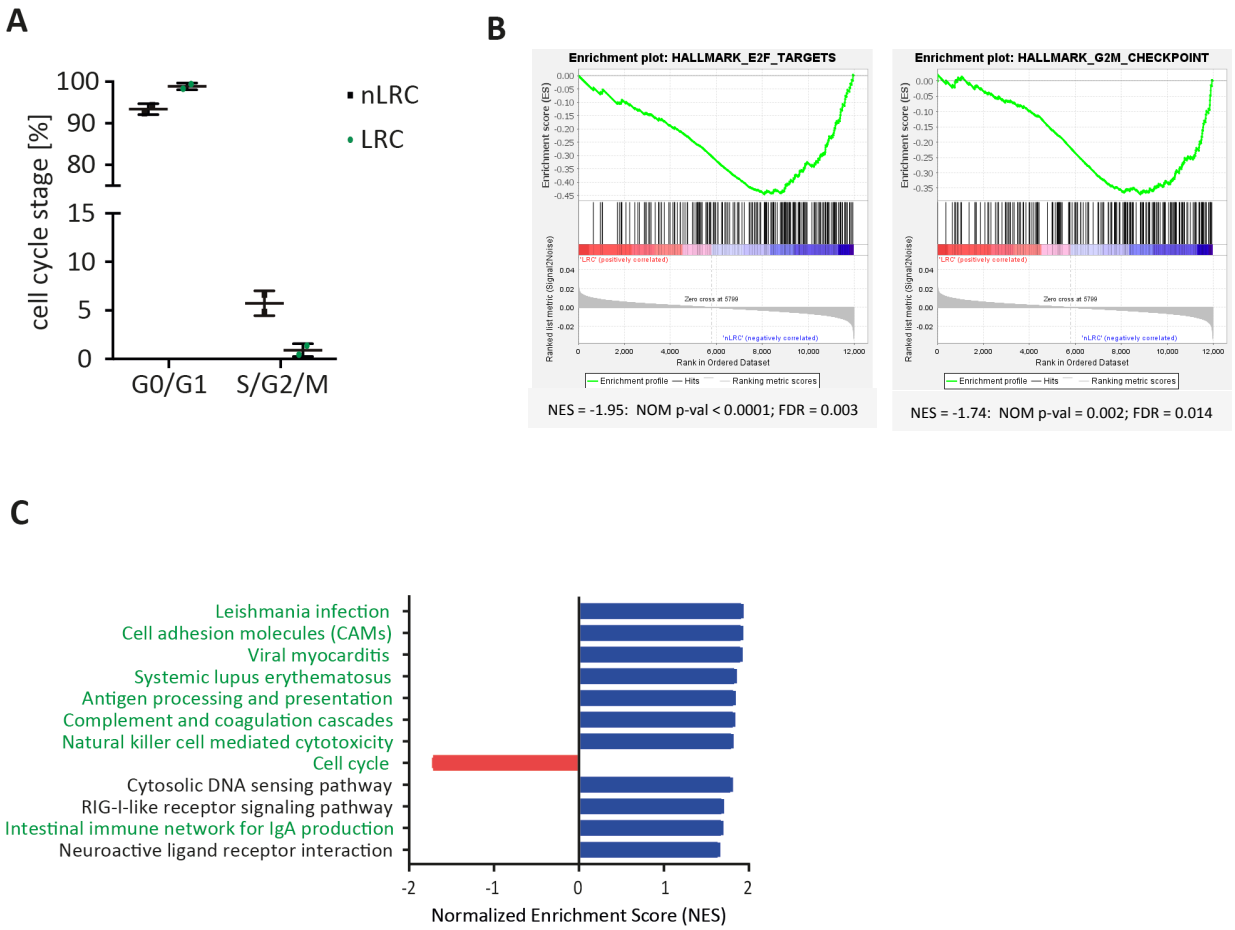

Figure S3 AML LRC are low cycling and resemble LRC from acute lymphoblastic leukemia (related to Figure **1**).

A Cell cycle analysis: 10^7 CFSE labeled AML-491 PDX cells were injected into two mice; cells were isolated at day 16, stained with Vibrant DyeCycle Violet and analyzed for CFSE content and cell cycle distribution by flow cytometry.

B Gene set enrichment analysis (GSEA): Comparison of LRC versus non-LRC by GSEA (hallmarks of cancer) demonstrate down regulation of the cell cycle activity pathways E2F target genes and G2M Checkpoint, indicating reduced proliferation.

C Significantly enriched KEGG pathways (nominal p-value ≤0.01) comparing LRC and nLRC of AML-393 and AML-491; KEGG pathways with concordant enrichment in both AML (new data here) and ALL (Ebinger et al, 2016) are marked in green.

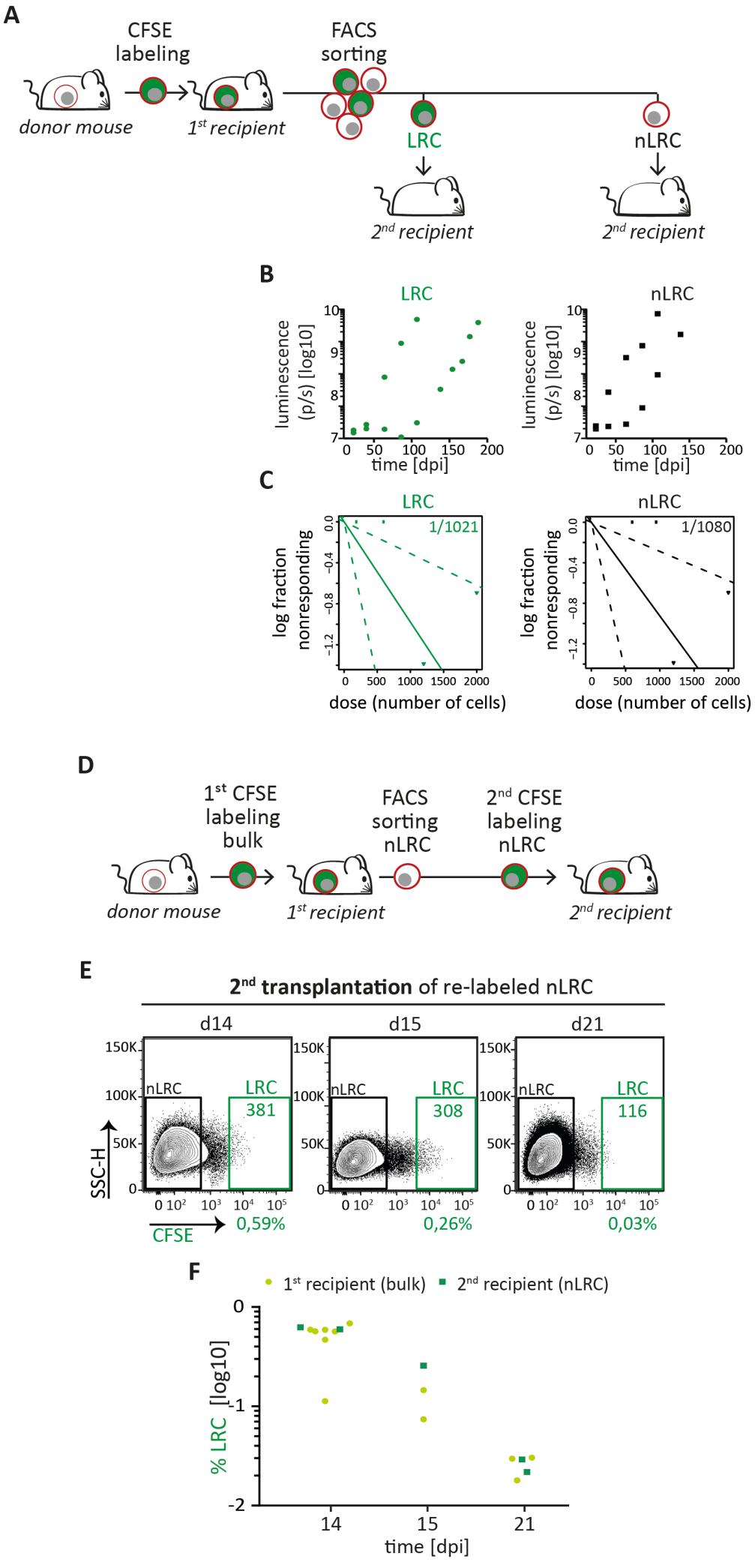
A
CFSE labeling
FACS sorting
donor mouse
1st recipient
LRC
nLRC
2nd recipient
2nd recipient
B
LRC
nLRC
luminescence (p/s) [log10]
time [dpi]
C
LRC
nLRC
1/1021
1/1080
log fraction nonresponding
dose (number of cells)
D
1st CFSE labeling bulk
FACS sorting nLRC
2nd CFSE labeling nLRC
donor mouse
1st recipient
2nd recipient
E
2nd transplantation of re-labeled nLRC
d14
d15
d21
nLRC
LRC
381
308
116
SSC-H
CFSE
0,59%
0,26%
0,03%
F
1st recipient (bulk)
2nd recipient (nLRC)
% LRC [log10]
time [dpi]

Figure S4 **AML PDX cells display reversible growth behavior, independently from stemness potential** (related to Figure **3,** additional sample AML-491)**.**

Experiments were performed and data depicted identically as in Figure **3**;

A Experimental procedure; AML-491 PDX cells were isolated from advanced disease donor mice (n=2 in two independent experiments), labeled with CFSE, and re-transplanted into first recipient mice. Fifteen days after injection, cells were re-isolated and sorted into LRC and non-LRC (nLRC) using the gates as described in Figure **1B** and re-injected into secondary recipient mice.

B Secondary recipient mice receiving either 1200 LRC or 1200 non-LRC (n=4) were monitored by in vivo imaging.

C LRC and non-LRC were re-injected into secondary recipient mice (n=11) in limiting dilutions at numbers as indicated in Table **S3**. Positive engraftment of PDX cells was determined by in vivo imaging and/or flow cytometry. LIC frequency was calculated using the ELDA software and is depicted +/- 95% confidence interval. No statistically significant difference between LIC frequency of LRC and non-LRC was found according to chi-square test (p=0.95).

D Experimental procedure; from first recipient mice (n=2 in 2 independent experiments) harboring CFSE stained cells, non-LRC were isolated at day 21, re-stained with CFSE and $1.9*10^6$ cells injected into secondary recipients; (n=5); Cells were re-isolated 14, 15 and 21 days later and LRC were quantified using gates as described in Figure **1B**. The experiment is technically unfeasible for LRC as the high number of cells needed cannot be generated.

E,F Representative dot plots (**E**) and quantification (**F**) of the percentage of LRC among all PDX cells isolated from secondary recipients is displayed (green squares). LRC of first recipient mice as determined in Figure **S2A** are shown for comparison (dots in light green).

See supplemental Table **S3** for additional data.

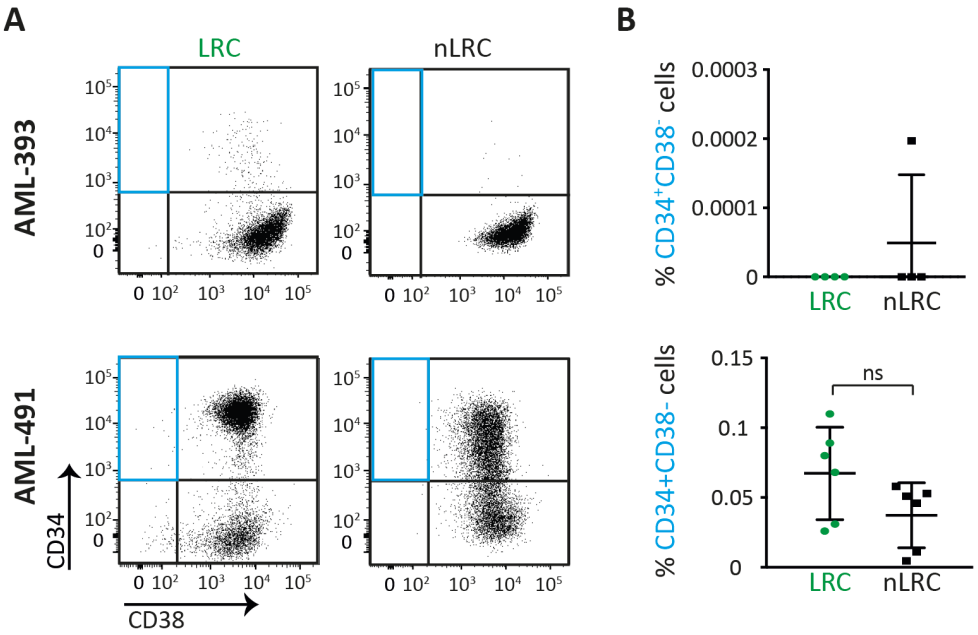

Figure S5 **Low-cycling cells are not enriched in immature cells**.

AML-393 and AML-491 PDX cells were isolated from full-blown donor mice, labeled with CFSE, and 10^7 cells were re-transplanted into first recipient mice. Ten (AML-393; n=4) or fourteen (AML-491; n=6) days after injection, cells were re-isolated, stained with CD34 and CD38 antibodies and percentage of CD34 and CD38 positive cells within the LRC and non-LRC compartment were analyzed by flow cytometry.

A representative dot plots

B percentage of CD34-positive and CD38-negative cells within the LRC and non-LRC compartment is depicted as mean+/-SD. Each dot/square represents one mouse;